MONITORING RESULTS OF AN INSTRUMENTED MSEW: COMPARISON WITH CURRENT PRACTICE

Robert Y. Liang
Professor
Civil Engineering Department
University of Akron
Auburn Science and Engineering Center,
Akron, OH 44325-3905
e-mail: rliang@uakron.edu.
Tel: (330) 972-7190
Fax: (330) 972-6020

Izzaldin M. Almoh'd(1)
Research Associate
Louisiana Transportation Research Center (LTRC)
Louisiana State University
4101 Gourrier Avenue, Baton Rouge, LA 70808
e-mail: aizzaldin@lsu.edu.
Tel.: (225) 767-9170.
Fax: (225) 767-9108.

Mustafa Al-Saleh
Former Grad. Stud. at the Univeristy of Akron,
Current Grad, Stud. at the Louis. State Univ.,
Civil Engineering Department,
e-mail: malsal1@lsu.edu

Number of words: 7500
Number of words in Abstract: 250

Keywords: Mechanically stabilized earth walls, field instrumentation, reinforcement axial force, working stress method, coherent gravity, Load and Resistance Factor Design.

November 2003

(1) Corresponding Author.

INSTRUMENTATION MONITORING RESULTS OF AN INSTRUMENTED REINFORCED EARTH WALL: COMPARISON WITH CURRENT PRACTICE

Robert Y. Liang, Izzaldin M. Almoh'd, and Mustafa Al-Saleh

ABSTARCT:

A field instrumentation and monitoring study on a 52 ft (15.8 m) high mechanically stabilized earth wall (MSEW) is presented in this paper. The field monitoring program was carried out on different sections along the wall representing three different wall heights and two geometries. The monitoring results pertaining to the reinforcement working forces, earth pressures at the base of the reinforced soils, and the wall deformations are presented. The magnitudes and locations of maximum axial forces measured in the reinforcement are discussed and compared to the predictions by the method adopted by the Federal Highway Administration (FHWA) and the Load and Resistance Factor Design (LRFD) method.

The comparisons between the field measurements and the design methods for the tallest section with straight backfill (simple geometry) indicated that the LRFD method predicted the reinforcement forces more closely than the FHWA adopted method. However, both methods failed to predict the locations and magnitudes of the maximum axial forces that developed in the reinforcement at the wing wall section (sections with three-dimensional sloping backfill). The geometry of the wall and backfill, the type of wall facing panels, and the inter-panel connections are believed to influence the deformation and settlement response of the reinforced earth wall. Based on the measured reinforcement-wall connection forces, the connection forces are shown to be dependent upon the depth of embedment and the shape of the line of limiting equilibrium.

The vertical pressure measurements showed deviations from those predictions by the three methods: Meyerhof, trapezoidal and the uniform distribution. These discrepancies can be attributed to the lack of knowledge of the influences of the wall facing element, and the frictional stresses that may have developed along the interface between the retained soil and the reinforced soil mass.

INTRODUCTION

The concept of earth reinforcement has been used intuitively for centuries where stiff inclusion members with strong tensile property are used to enhance the behavior of deformable weak-in-tension soils. Vidal (*1, 2*) was the first to introduce the modern concept of soil reinforcement in an interesting case study in France. Since then, worldwide research and demonstration projects on soil reinforcement have continuously evolved under the sponsorship of several agencies, such as: The U.S. Department of Transportation (*3*), United Kingdom Transportation and Road Research Laboratory (TRRL) (*4*), as well as various leading agencies and laboratories in France (*5*).

Currently, there are many methods (*6 to 12*) that can be used for the analysis and design of mechanically stabilized earth walls (MSEW). In the United States, the design/analysis of MSEW has been based on the allowable stress design (ASD) method, the load factor design (LFD) method, or the recently developed load and resistance factor design (LRFD) method. The concept of working stress has been widely described and recognized (*11*, *13*, *14*, *15*, *16*). Yet, most of the popular methods are empirical in nature and are primarily based on model tests results (*12*). Despite the fact that the existing design methods may provide conservative design results, they have failed to clearly demonstrate the inherent advantages of the optimum reinforcement distributions upon which the design is based. This could be attributed to the simplifying assumptions and, in some instances, the predetermined reinforcement density and dimensions that would often lead to unnecessary conservatisms. Some of the drawbacks of existing analysis methods include the simplifying assumptions regarding the strain compatibility between the soil and the reinforcement, friction free interface between soil layers, and treating the reinforced soil mass as a rigid block. Furthermore, the added confinement due to the stiffness of the reinforcement, as well as reinforcement layout and wall facing material and geometry were not considered in the existing analysis methods. A study conducted by Collin (*17*) indicated that the predicted reinforcement forces by the Coherent Gravity method (*6, 12*) failed to approximate the actual measured forces. Lee et al. (*18*) also reported the failure of four walls in Tennessee, designed using the Coherent Gravity method. Field validation of some of the values and assumptions for the design variables pertaining to MSEW is still needed. Abu-Hejleh et al. (19), in one of the most recent researches, assessed the efficiency of the design method and the assumptions involved in geosynthetic reinforced soil (GRS) abutments. A field instrumentation program to monitor the reinforcement forces, connection forces, lateral pressures acting on the wall facing, and vertical earth pressures within the reinforced soil mass has been conducted leading to significant understanding of GRS behavior.

The load and resistance factor design (LRFD) method has been adopted by the American Association of State Highway and Transportation Officials (AASHTO) since 1994 (*20)*. The LRFD approach is a probabilistic approach which considers the variability in the material properties and loads. Load and resistance factors are used to amplify the loads and reduce the resistance of the structure, respectively. Calibration of the load and resistance factors for different structures and load conditions has been one of the ongoing challenges for researchers (*21, 22*). The use of LRFD method in the design of MSEW and the length of calculations involved have been reported in (*22*).

In this paper, both the FHWA approved approach and the LRFD method will be compared with the field measurements of an MSEW constructed in Muskingum County, Ohio.

MSEW AT MUSKINGUM COUNTY, OHIO

This MSEW is about 700 ft (213.4 m) long, with 22 HP14 x 74 point bearing piles located at 3 ft (0.91 m) behind the wall facing to support the bridge footings. PVC pile sleeves were used to minimize the skin friction along the pile and to facilitate transfer of the bridge loads to the hard subsurface strata. Schematic views of the MSEW are depicted in Figure 1.

The reinforced backfill material used for the project was graded sand (SW) compacted to a minimum of 95% of the maximum Proctor's unit weight (ASTM D-698). This corresponded to a field dry unit weight of 110 pcf and an angle of internal friction of 34^o obtained from direct shear tests. The retained backfill was cohesionless soil with an angle of internal friction of 30^o and a dry unit weight of 110 pcf. A 4 ft (1.22 m) thick layer of DOT Item 304 backfill soil was used to replace the original top soil at the construction site. Perforated corrugated plastic pipes, 6 inches (15.2 cm) in diameter, were placed on top of the replaced foundation soils, both behind the wall facing and at the far end of the reinforced soil mass.

The MSEW used 2 inch (5 cm) wide, and 0.16 inch (4 mm) thick galvanized steel reinforcement straps and 5 ft x 5 ft (1.5 m x 1.5 m) precast concrete segmental cruciform facing panels. The vertical spacing of reinforcement straps was 2.5 ft (76 cm), and the horizontal spacing was varied from 1.0 ft (30 cm) at the bottom of the wall to 3.33 ft (1.0 m) at the top. The lengths of reinforcements at each wall section were uniform throughout the depth. However, they were varied according to wall height as follow: 36 ft (11 m), 20 ft (6.1 m), and 16 ft (4.9 m), for the 52 ft (15.8 m), 30 ft (9.1 m), and 20 ft (6.1 m) wall heights, respectively. The elastic modulus for the reinforcement was tested in the laboratory to be 28×10^6 psi (193 MPa).

INTRUMENTATION PLAN

The instrumentation program was designed to monitor the axial forces in the reinforcement, the vertical earth pressures at the base of the reinforced soil mass, the lateral earth pressures acting on the wall facing, and the wall facing movements. Four sections of the wall were instrumented: two 52 ft (15.8 m) high sections, denoted as sections A and B, close to the bridge median, and 30 ft (9.1 m) and 20 ft (6.1 m) high sections, denoted as sections C and D, respectively, located away from the median within the sloping wing-wall. The locations of these sections are indicated in Figure 1.

Nine of the 21 reinforcing straps in each section A and B were instrumented with vibrating wire strain gages at different locations along the strap to provide adequate measurements for the distribution of the reinforcement forces. Four pressure cells were installed beneath these sections at horizontal distances of 5 ft, 10 ft, 20 and 30 ft (1.5, 3, 6.1, and 9.1 m) from the wall facing. In sections C and D, seven and six reinforcement straps were instrumented with strain gages, respectively. The instrumentation plans for all sections are depicted in Figures 2a, b and c, for the 50 ft, 30 ft, and 20 ft wall sections, respectively.

Vibrating wire strain gages (Geokon VK-4150), shown in Figure 3a, were used to monitor the reinforcement working forces during and after construction. As shown in Figure 3, the instrumented reinforcement straps were carefully placed and connected to the wall facing. The initial readings were made within the first day of installation under about 3 to 4 inches (7.6 to 10 cm) thick soil cover. The pressure produced by the soil cover was used to eliminate the noise of the strain gages. The earth pressure cells were Geokon VW-4800, and installed along the foundation of sections A and B as shown in Figure 3c. The MSEW and bridge structures at

the end of construction are shown in Figure 3d. More details about the entire instrumentation plan and the monitoring results are provided in (*23*, *24*).

All gages and sensors were connected to 16/32 channel multiplexers, which were in turn connected to CR10X dataloggers. Data sampling frequency was set to 2 minute intervals during wall construction. By the end of construction, the sampling intervals were set to 2 hours.

RESULTS AND DISCUSSION

Reinforcement Axial Forces

The average strains of the two strain gages mounted at the two sides of the reinforcement straps were used to compute the axial forces. The measurements during wall construction and after placing surface surcharge will be presented separately in the following sections.

Forces During Construction

Since sections A and B are both 52 ft high sections close to the median area, the average monitoring results for those two sections are used to represent the field performance. The measured reinforcement axial forces at different soil overburden heights during construction of the 52 ft (15.8 m) high wall section are shown in Figure 4. The measured maximum axial force in the reinforcement was observed in the straps located at 6.25 ft (1.9 m) and 11.25 ft (3.4 m) above the leveling pad, corresponding to 48.25 ft (17.4 m) and 41.25 ft (12.6 m) below the wall copping, respectively. The maximum forces measured in these straps at the end of construction were higher than the maximum force measured in the bottom reinforcement layer located at 1.25 ft (0.38 m) above the leveling pad. This is considered to be the result of the earth pressure exerted by the 5 ft (1.5 m) of backfill placed in the front of the wall, shown in Figure 2.

The measured axial force profiles for the instrumented straps in the 30 ft (9.1 m) high section are shown in Figure 5. The maximum reinforcement forces at the completion of wall construction were observed in the third reinforcement layer from the leveling pad. The presence of backfill outside the wall again contributed to this behavior. The reinforcement force profiles for the 20 ft (6.1 m) high section are presented in Figure 6. Finally, Table 1 provides a summary for the maximum forces measured in the instrumented reinforcement straps at the end of wall construction for all instrumented wall sections.

To show the development of reinforcement forces as a function of the overburden height, Figures 7a and 7b are plotted to represent the measurements of the axial forces in two typical reinforcement layers in sections A and C, respectively. Based on these figures, it can be observed that the measured forces in most of the strain gages have increased linearly with increasing overburden soil height up to 10 ft (3 m). Above 10 ft (3 m) of fill, the maximum reinforcement forces were relatively easier to locate. This phenomenon may suggest possible relaxation in the lateral support (confinement) at different overburden heights. The loss of lateral confinement (support) seems to increase with increasing overburden height. The phenomenon of the loss of lateral confinement as the overburden height exceeds certain limiting values may provide rationale for the non-linear interrelationship between the reinforcement-soil interface friction and the soil overburden height.

For majority of the instrumented straps, the locations of the maximum axial force can be observed. The loci of maximum tensile forces would approximate the line of limiting equilibrium (likely failure surface). However, some of the axial force profiles have shown more

than one peak in the axial force profiles. It is reasoned that local deflections of the slender reinforcement may have changed the direction (sign) of the friction stresses along parts of the reinforcement, thus producing local peak axial forces.

The reinforcement-wall connection forces are calculated using the measured reinforcement strains in the strain gages located at 1-ft from the wall facing. The connection forces and the ratios between the connection forces and the maximum reinforcement forces are shown in Figures 8a and 8b, respectively. Referring to Figure 8a, the connection forces are shown to be related to the overburden pressure by a factor ranging from 0.25 up to 0.75. The ratios, shown in Figure 8b, vary with the embedment depth. Theses variations are influenced by the shape of the line of limiting equilibrium, which defines the locations of the maximum reinforcement forces. At the upper part of the wall, the locations of the reinforcement maximum forces are away from the wall facing, thus causing the connection forces to be as low as 25% of the maximum axial forces. At the lower portion of the wall, the locations of the maximum axial forces become closer to the wall, thus increasing the connection forces. At the bottom reinforcement layer, the connection force becomes approximately equal to the maximum force developed in the reinforcement. Accordingly, the connection forces should be considered in the design of MSEW as a function of the overburden depth of the reinforcement and the shape of the line of limiting equilibrium. The ratio of the connection force over the maximum force reaches a maximum value equal to 1.0 at the bottom reinforcement layer, and a minimum value of about 0.25 at the top of the wall.

Effect of Surcharge Load

By the end of wall construction and reinforced soil backfilling, other construction activities occurred at the site, including: bridge structure construction, final grading, and construction of the concrete pavement. It is estimated that these activities may have introduced an equivalent of surface surcharge load of about 1.0 ksf (48 kPa) on top of the reinforced soil mass. Using the simple trapezoidal rule, the equivalent dead-load surcharge would approximately be 0.6 ksf (28.8 kPa) at the depth 5 ft (1.5 m) below the top of the reinforced soil.

The measured additional reinforcement forces due to the estimated surcharge load are summarized in Table 1. All four instrumented sections have been influenced by the bridge construction and grading activities. In the 52 ft (15.8 m) high section, the lower reinforcement layers are influenced by the surface load more than the upper layers. It is reasoned that the piles behind the MSEW facings may have reduced the lateral movement at the upper portion of the wall, thus restraining further increase in reinforcement forces. On the other hand, more movements in the lower portion of the wall may have contributed to higher additional forces in the lower level reinforcements. The two wing-wall sections (sections C and D), located away from these activities, are also influenced by the surface surcharge loads from the bridge due to the three-dimensional geometry of these sections.

Comparison with Current Practice

The measured maximum reinforcement forces are compared with the FHWA approved design approach and the LRFD method in Figures 9a, 9b, and 9c, for sections A and B, section C, and section D, respectively. As can be seen from these figures, both methods have overestimated the forces in the 50 ft and 30 high sections, and underestimated the reinforcement forces in section D (20 ft high section). The overestimation of the forces in the

50 ft and 30 ft sections may be due to the presence of the piles close to those sections and the conservatism of design of the as-built reinforcement spacing and lengths. The underestimate of the reinforcement forces in the wing-wall sections (sections C and D) could be attributed to the three dimensional geometry of these wing-wall sections. It is hypothesized that both torsional and flexural stresses are likely to develop in the reinforcement layers, especially near the reinforcement-wall connections. This notion can be supported by examining Figure 10, where the maximum reinforcement forces in section D were located near 2.5 ft (0.76 m) away from the wall facing (Figure 10c). For sections A and B, shown in Figure 10a, the location of the maximum tensile forces in the reinforcement was closely reflected by the FHWA envelope. For section C, shown in Figure 10b, the likely failure surface appears to conform with the two-part wedge failure surface extending through the foundation soil, as suggested by Romstad et al. (*25*).

Deformations of Wall Facing

Point surveys were made on a monthly schedule along the height of the wall at the outside facing of each of the instrumented sections. These measurements provided information of the wall panel movements in all three directions: vertical settlement and lateral deflections.

Settlement of Wall Facing

The settlement of the wall facing was obtained from the differences in the elevations measured at the lowest survey point at each wall section at different times during and after construction. However, it was not possible to install the survey points on the first panel above the leveling pad, since it was located under the ground surface required for minimum embedment. The anticipated joint contraction due to cumulative panel weights was estimated to be below 0.20 inch (5 mm) and was subtracted from the movement measurements.

The approximate settlement of the wall facing for sections A, C, and D are shown in Figure 11a. The settlement curve for section A has shown upward movements in the second survey reading (on October 21, 2000). This is due to pile driving at the site, which caused soil particles to move upward (heave). The settlements at the two wing-wall sections (sections C and D) are shown to be considerably higher than that at the 52 ft (15.8 m) high wall section (Section A). This is mainly attributed to the weaker subsurface conditions, as well as the influence of the piles driven in sections A and B. The maximum differential settlement of the wall was found to be less than 0.3 % of the wall height, thus satisfying the FHWA design specifications.

Lateral Wall Deformation

The lateral deflections of the wall facing have been calculated and projected into the normal and parallel directions for sections A and C. The lateral deflections in the direction normal to the wall are plotted in Figures 11b and 11c, for wall sections A and C, respectively. It can be seen that the maximum lateral movements of the wall were 0.45 inch (11.4 mm) and 1.7 inches (43.2 mm) for sections A and C, respectively. Based on the FHWA Design Manual, a limiting value for the lateral wall deflection would be the wall height divided by 250 for the case of inextensible reinforcement. This corresponds to the maximum allowable deflections of about 2.4 inch (61 mm) and 1.44 inch (36.6 mm) for sections A and C, respectively. Accordingly, the maximum lateral deflections observed at section A were well within the FHWA preferred limits; whereas, the deflections of section C were a little over limit.

Vertical Pressure Measurements

The measured vertical earth pressures at the base of reinforced soil mass during wall construction are shown in Figure 12a, where each curve corresponds to a different soil overburden height. A maximum vertical earth pressure was measured by the pressure cell located at 5 ft (1.5 m) from the wall facing. This can be attributed to a number of factors, such as: the external horizontal pressure exerted by the retained soil mass, the mobilized frictional stresses along the interface between the reinforcement and the soil, and the reinforcement wall connections. On the other hand, the minimum vertical earth pressure was observed at about 10 ft (3 m) from the wall facing, which corresponds to the locations of maximum axial forces in the reinforcement in the upper portion of the wall (about 1/3 the length of reinforcement). As shown in Figure 12b, the maximum and minimum pressures are equal to 167% and 65% of the geostatic soil pressure (i.e., 1.67 γh and 0.65 γh; where $\gamma$is the unit weight and h is the overburden height). The pressure distribution is influenced by the following factors: flexibility of the structure, pressure exerted by the retained mass, wall-soil and wall-connection forces, and the intensity and layout of reinforcements. Depending on the reinforcement layout, the lateral confinement will vary accordingly (i.e., reducing the reinforcement intensity reduces the lateral confinement). This will, in turn, reduce the vertical pressure. The soil-wall interface friction, on the other hand, will increase the vertical pressure close to the wall facing. These two factors, together, can be used to explain for the shape of the pressure distributions (*23, 24*).

Based on the measured vertical earth pressure profile along the base of the reinforced soil mass, the eccentricity, e, in the base pressure is estimated to be 3.8% of the total width, B, of the reinforced soil mass. This value is less than the limiting value for overturning stability ($e \leq B/6$).

A comparison between the measured pressure distribution and the commonly used distributions: Meyerhof, Trapezoidal, and uniform distributions, is provided in Figure 12c. The vertical earth pressures close to the side of the retained soil mass is higher than those predicted by the trapezoidal and the Meyerhof's distributions. The three vertical pressure distribution functions have the common shortcomings, such as, not accommodating for the influence of the wall facing connections and wall facing materials, the interface friction between the retained and the reinforced soil masses, and the assumption of a rigid reinforced soil mass. There is a need for a reconsideration of the vertical earth pressure distribution function and an investigation of the possible influences of the wall facing-soil and wall facing-reinforcement interactions on the vertical earth pressure distribution.

SUMMARY AND CONCLUSIONS

The results of field instrumentation and monitoring program of an MSEW in Ohio during and after construction were presented. The monitoring data included the reinforcement working forces, the wall facing deformations, and the vertical earth pressure distribution along the base of the reinforced soil mass. The field measurements of reinforcement working forces were compared with the FHWA adopted approach (*12*) and the LRFD method (*20, 22*). Based on these comparisons, the LRFD method was found to be closer to the measured field response and not as conservative as the FHWA adopted approach. However, for wall sections with sloping backfill (three-dimensional geometries), both methods showed greater differences from those observed in the field. Part of the reasons for such observed discrepancies can be attributed to the inability of the current methods to accommodate the influences of the geometry of the

wall (such as wing-walls), the stiffness of the wall facing, and the torsional and flexural stresses developed at the reinforcement-wall connections. Based on the measured reinforcement-wall connection forces, it was shown that the ratio of the connection force to the maximum axial force varied with the depth of reinforcement elevation as well as the shape of the line of limiting equilibrium. A maximum ratio of unity (1.0) was obtained for the bottom reinforcement layer; however, the ratios were approximately equal to 0.25 for the reinforcement layers at the upper part of the wall.

Based on the measurements of settlements and lateral movements of wall facing, it was shown that the geometry of the wall and backfill, and the type of wall-reinforcement connection could have contributed to the various patterns of deformation response of the MSEW. The differential settlements and the lateral movements of the wall were shown to be interrelated. Accordingly, an understanding of the influence of the wall facing stiffness (facing type and panel connection), and the wall geometry is essential to the evaluation of the deformation response of the MSEW. The presence of the driven point-bearing piles behind the wall facing was shown to be advantageous, because they had effectively reduced the reinforcement forces and the wall deformations.

The vertical pressure measurements showed large variations from the predictions of the three distribution methods: Meyerhof, trapezoidal, and the uniform distribution. These discrepancies can be attributed to the lack of knowledge of the influences of the wall facing element, and the frictional stresses that may have developed along the interface between the retained soil and the reinforced soil mass.

ACKNOWLEDGMENT

The authors gratefully acknowledge the support of Jawdat Siddiqi of the Ohio Department of Transportation (ODOT). The results presented herein are part of research project sponsored by ODOT.

REFERENCES

1. Vidal, H. La terre arm`ee'. Annls L'Inst. Tech. De Batiment et des Travaux Publics, S`erie Materiaux 30, Supplement No. 223-4, July-August, 1966.
2. Vidal, H. The Principle of Reinforced Earth. Transportation Research Record, 282, 1969, 1-16.
3. Walkinshaw, J. L. Reinforced Earth Coonstruction. Department of Transportation FHWA Region 15. Demonstration Project No. 18, 1975.
4. Murray, R. T. Research at TRRL to Develop Design Criteria for Reinforced Earth. Symp. Reinforced Earth and other Composite Soil Techniques. Heriot-Watt University, TRRL Sup. 457, 1977.
5. Schlosser, F.M. Experience on Reinforced Earth in France. Symp. Reinforced Earth and other Composite Soil Techniques, Heriot-Watt University, TRRL Sup. 457, 1977.
6. Mitchell, J.K., and Villet, W.C.B. Reinforcement of Earth Slopes and Embankments. NCHRP Report No. 290, Transportation Research Board, Washington D. C., 1987, pp.323.

7. Leshchinsky, D., and Perry, E.B. A design procedure for geotextile-reinforced walls. Proceeding of Geosynthetics'87, New Orleans, LA, 1987.
8. Jewel, R.A. Reinforced soil wall analysis and design. Proceedings of the NATO Advanced Research Workshop on Application of Polymer Reinforcement in Soil Retaining Structures, 1990.
9. Bonaparte, R., and Schmertmann, G. Reinforcement extensibility in reinforced soil and soil wall design. Proceedings of the NATO Advanced Research Workshop on Application of Polymer Reinforcement in Soil Retaining Structures, 1988.
10. Gourc, J.P, Ratel, A., Gotteland Ph. Design of reinforced soil retaining walls: analysis and comparison of existing design methods and proposal for a new approach. Proceedings of the NATO Advanced Research Workshop on Application of Polymer Reinforcement in Soil Retaining Structures, 1990.
11. Christopher, B.R. Deformation response and wall stiffness in relation to reinforced soil wall design. Ph.D. dissertation, Purdue University, 1993.
12. Elias, V., and Christopher, B. R. Mechanically stabilized earth walls and reinforced soil slopes design and construction guidelines. Report No. FHWA-SA-96-071, FHWA, Washington, D.C. 1986.
13. Schlosser, F. M. Mechanically stabilized retaining structures in Europe- Design and Performance of Earth retaining Structure. Edited by Philip C. Lambe and Lawrence A. Hansen, New York, 1990.
14. Jewel, R.A. Reinforced soil wall analysis and design. Proceedings of the NATO Advanced research Workshop on Application of Polymer Reinforcement in Soil retaining Structures, 1985.
15. Juran, I. In-situ ground reinforcement –soil nailing. ASCE Geotechnical Special Publication N0. 12, 1987.
16. Liang Y. R., Feng, Y., and Vitton, S. J. Displacement based stability analysis for anchor reinforced slope. Soils and Foundations, Vol. 38, No.2, Japanese Geotechnical Society, 1998, pp. 27-39.
17. Collin, J. G. Earth Wall Design. Doctoral Thesis submitted to University of California, Berkeley, California, 1986, 440 p.
18. Lee, K., Jones, C. J. F. P., Sullivan, W. R., and Trolinger, W. 1994. Failure and deformation of four reinforced soil walls in eastern tennessee. Geotechnique 44, No. 3, 397-426.
19. Abu-Hejleh, N.M., Zornberg, J.G., Elias, V., Watcharamonthein, J., "Design assessment of the Founders/Meadows GRS abutment structure", TRB 2003 Annual Meeting CD-ROM.
20. AASHTO. LRFD Bridge Design Specifications, 1st edition, Washington, DC: American Association of State Highway and Transportation Officers, 1994.
21. Nowak, AS. Calibration of LRFD bridge design code. Final Report. Ann Arbor, MI: Department of Civil and Environmental Engineering, the University of Michigan, 1993.
22. Chen, Y. Practical analysis and design of mechanically stabilized earth walls-I. Design philosophy and procedures. Engineering Structures, 22, 2000, pp. 793-808.

23. Liang, Y. MSE wall and reinforcement testing at MUS-16 bridge site. Report to be submitted to the Ohio-DOT, FHWA, U.S. Department of Transportation, 2003.
24. Almoh'd, I. Almoh'd. A new method for the design and analysis of reinforced earth walls. A PhD thesis submitted to the University of Akron, Ohio, 2003.
25. Romstad, K.M., Al-Yassin, Z., Herrmann, L.R., and Shen, C.K. Stability analysis of reinforced earth retaining structures. Proc. ASCE Symposium on Earth Reinforcement, Pittsburge, Penn., 1978, pp.685-713.

LIST OF FIGURES

TABLE 1 Measure Maximum Reinforcement Forces at the End of Construction and After Application of Surface Surcharge Loads.

No.	Overburden depth ft	Max. Force kip/ft			Force increment* kip/ft
		Measured	FHWA	LRFD	
52 ft high (sections A & B)					
S9	3.75	0.37	0.32	0.48	0.13
S8	11.25	0.40	1.12	1.32	0.1
S7	18.75	0.71	1.50	1.90	0.49
S6	23.75	1.28	2.0	2.50	0.62
S5	28.75	2.92	2.40	2.92	NA
S4	36.25	1.64	3.30	3.75	0.26
S3	41.25	2.09	3.78	4.30	1.01
S2	46.25	2.24	4.3	4.75	1.06
S1	51.25	2.29	4.75	5.22	NA
30 ft high (section C)					
S7C	3.25	0.42	0.40	0.60	0.78
S6C	5.75	0.81	0.75	0.90	NA
S5C	8.25	0.89	1.08	1.25	0.51
S4C	13.25	1.09	1.60	1.60	0.21
S3C	18.25	1.33	1.85	1.93	0.17
S2C	23.25	2.4	2.20	2.40	NA
S1C	28.25	1.77	2.65	2.90	0.63
20 ft high (section D)					
S6D	1.25	NA			NA
S5D	3.75	0.8	0.50	0.50	0.4
S4D	6.25	1.6	0.80	0.80	0.8
S3D	11.25	1.3	1.35	1.45	0.5
S2D	16.25	2.6	1.75	1.85	1.3
S1D	18.8	1.7	1.92	2.09	0.5

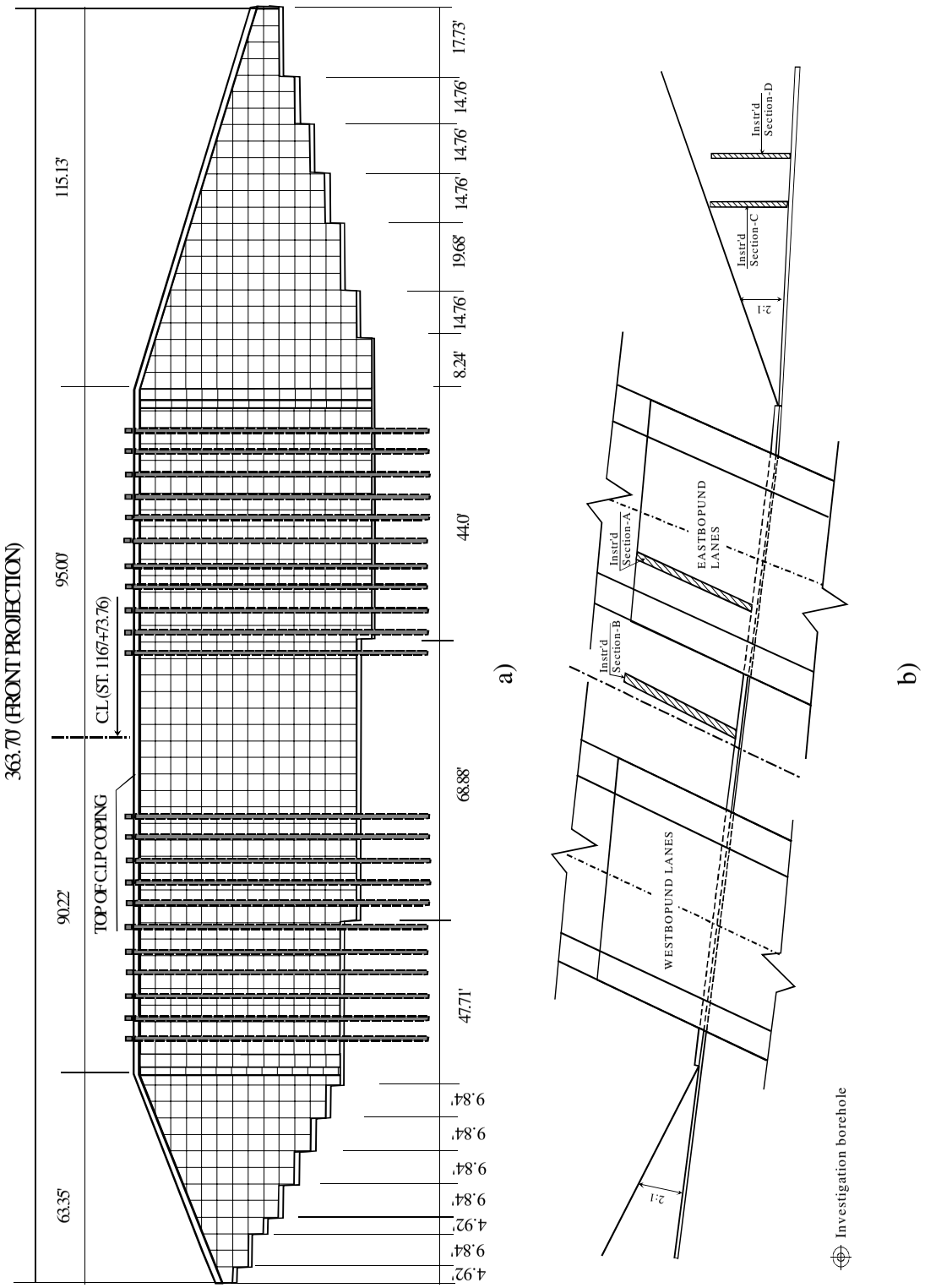

Figure 1 Schematics of the instrumented MSE wall: a) front projection, and b) plan view

TRB 2004 Annual Meeting CD-ROM

Paper revised from original submittal.

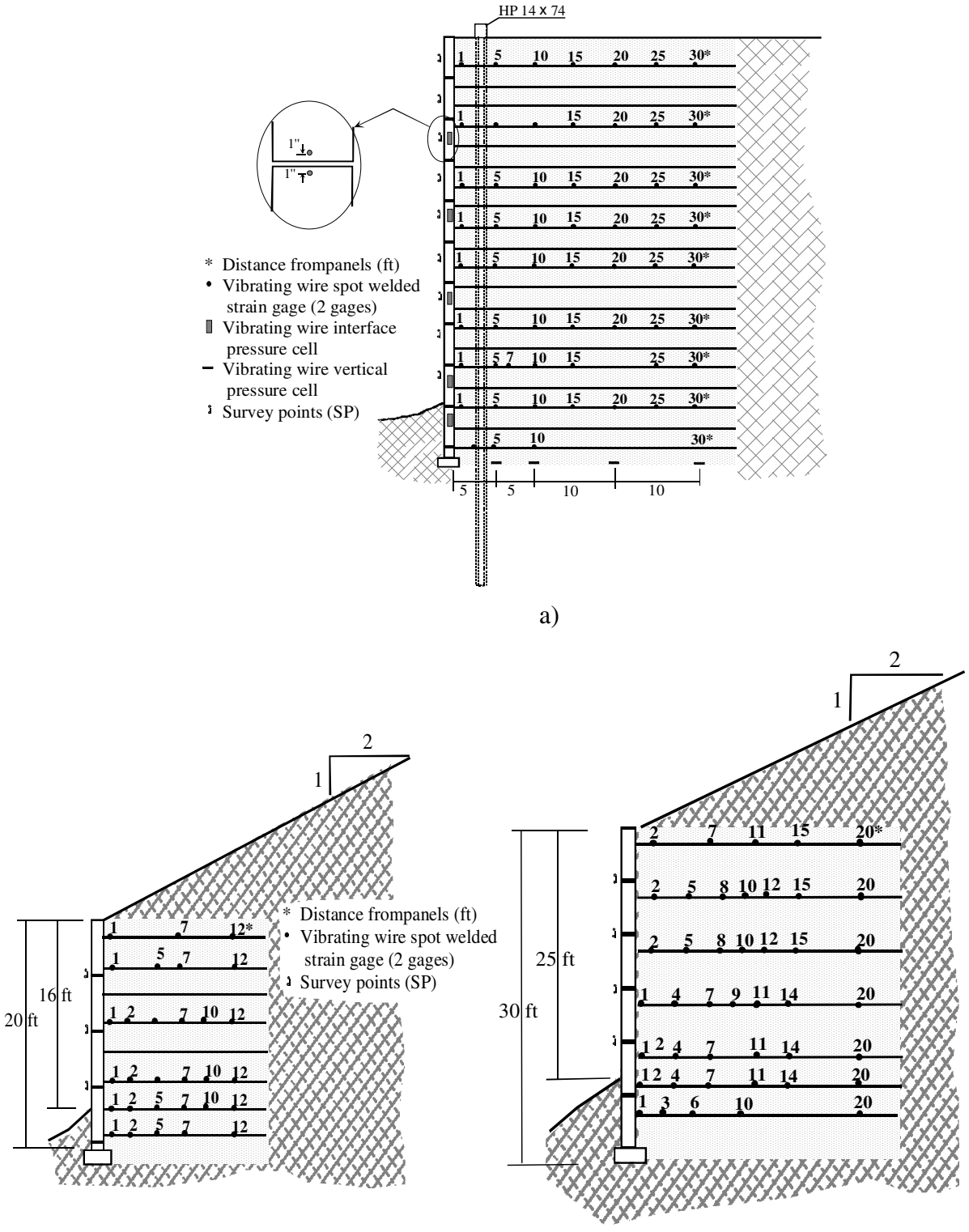

Figure 2 Instrumentation plan for: a) 52-ft high sections (sections A and B), b) 30 ft high section (section C), and c) 20 ft high section (section D).

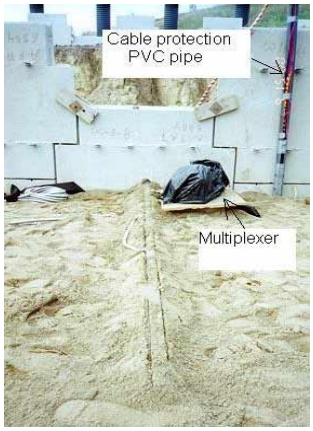

a)

b) c)

Figure 3 a) Installation of strain gages and instrumented reinforcement strap, b) installation of pressure cells, and c) MSE abutment walls and bridge at the end of construction.

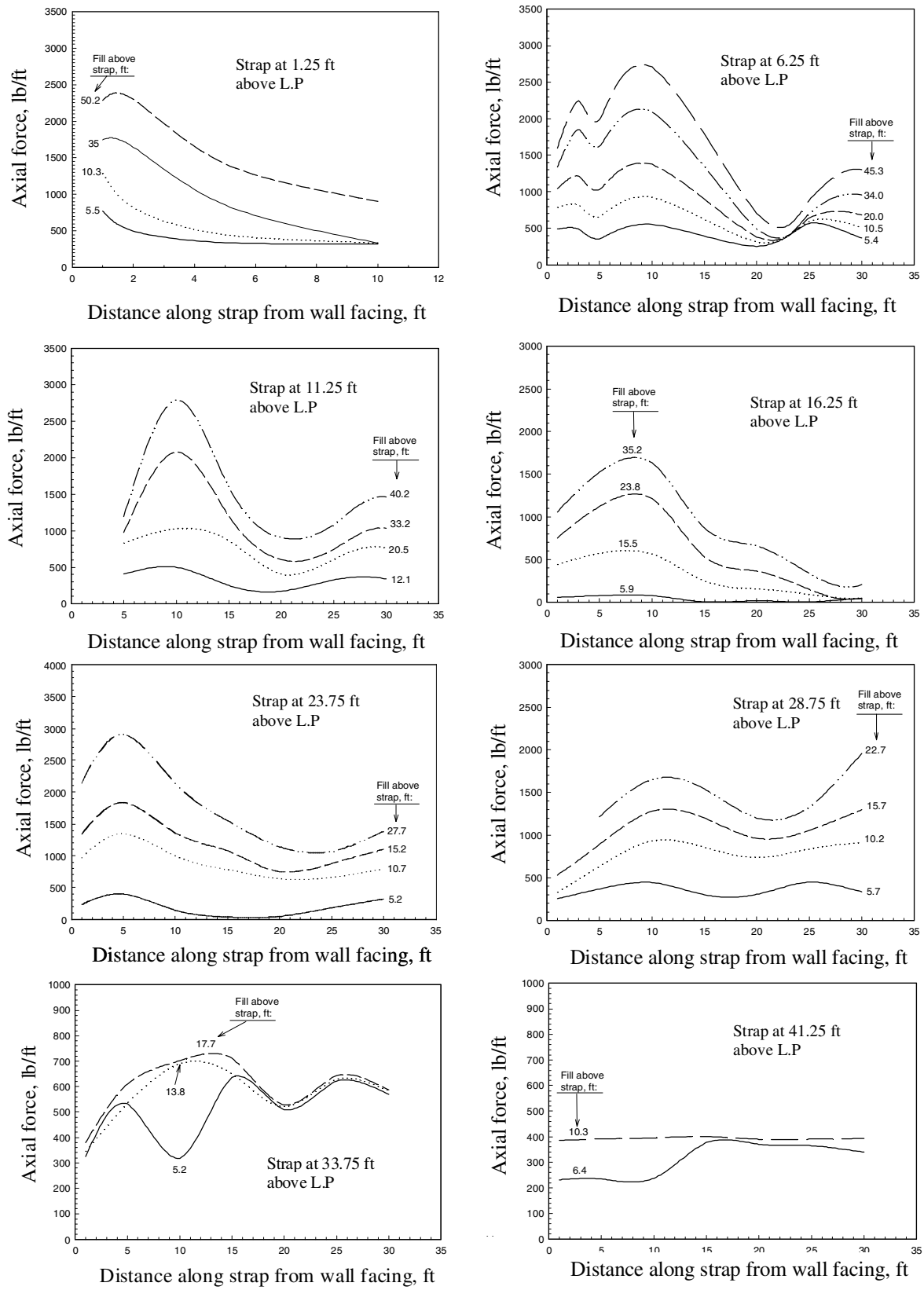

Figure 4 Measured force profiles for the instrumented reinforcement straps located at different elevations above the leveling pad (L.P) in the 52 ft high section.

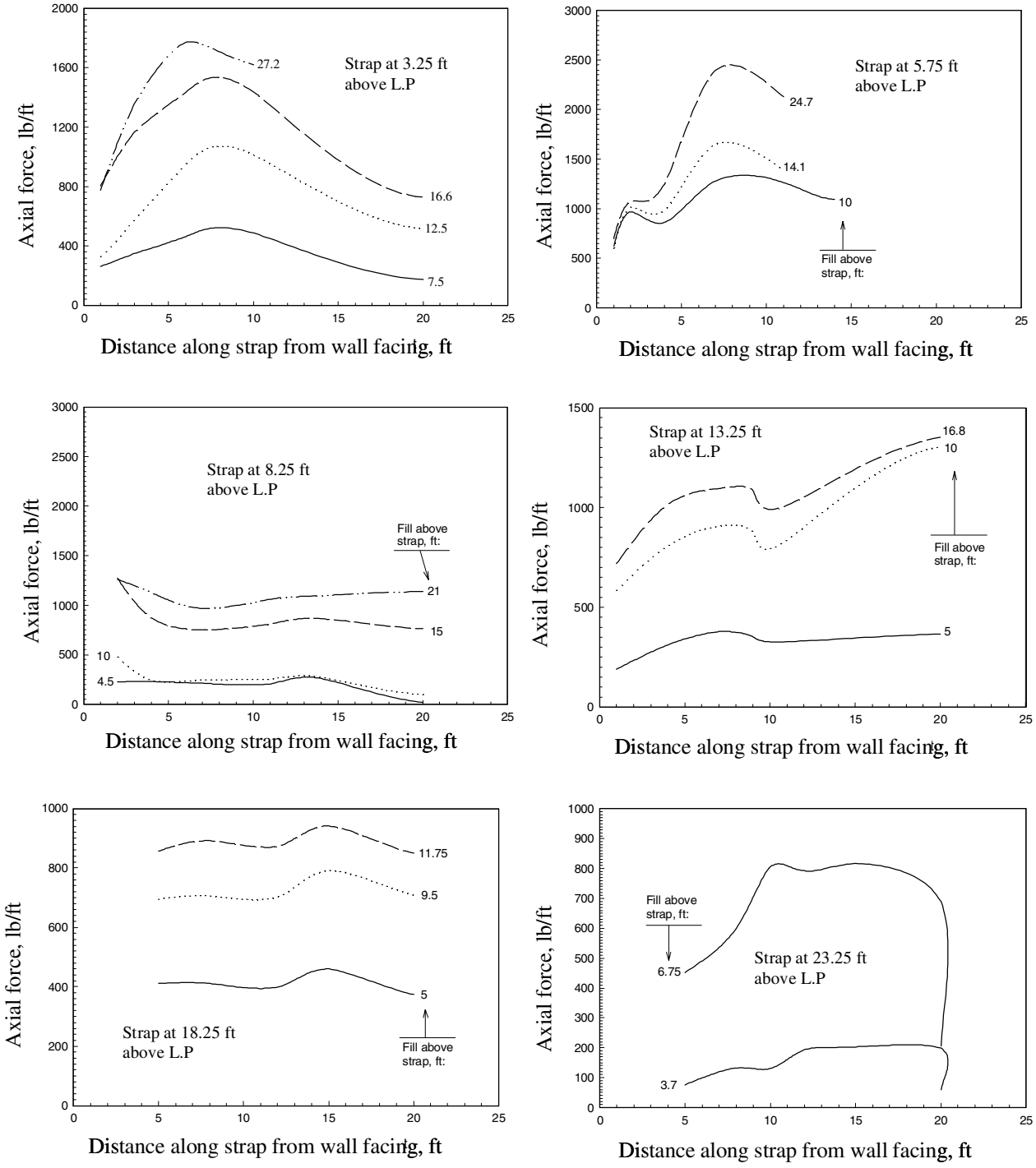

Figure 5 Measured force profiles for the instrumented reinforcement straps located at different elevations above the leveling pad (L.P) in the 30 ft high section.

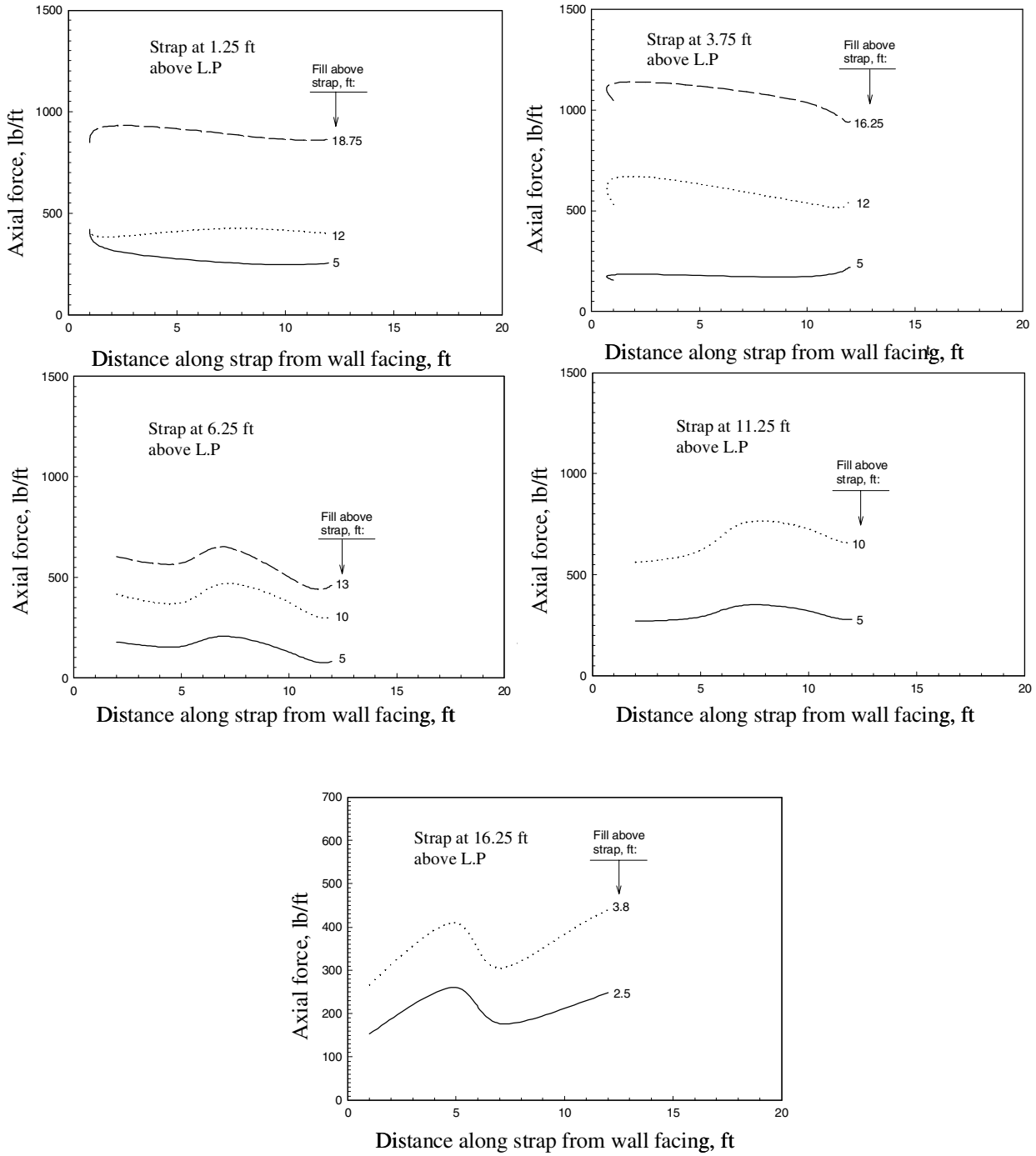

Figure 6 Measured force profiles for instrumented straps located at different elevations above the leveling pad (L.P) in the 20 ft high section.

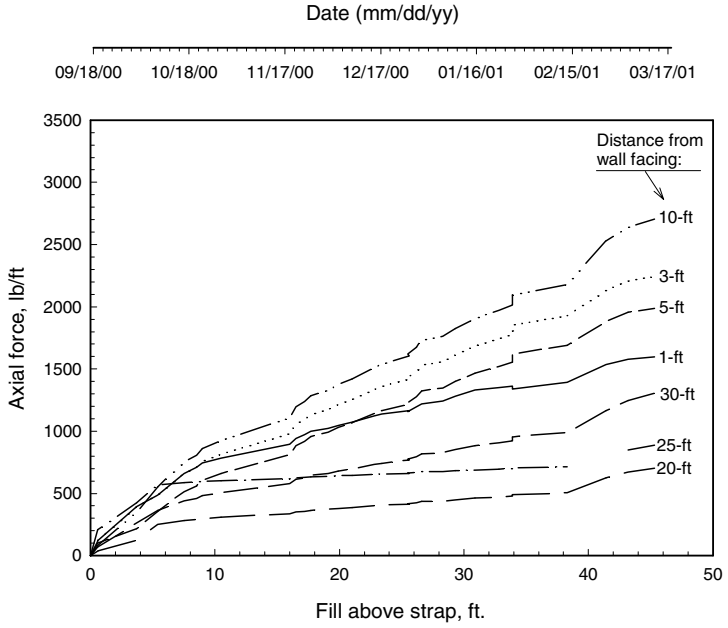

a)

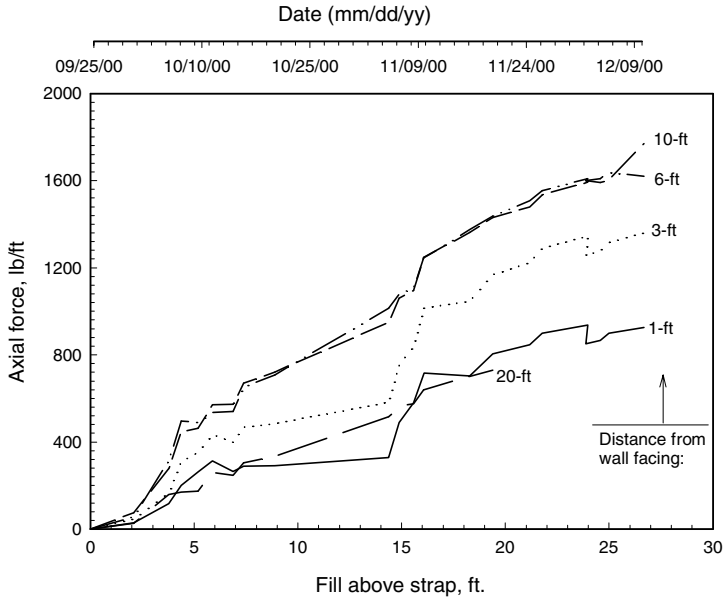

b)

Figure 7 Measured reinforcement axial forces at different locations along the reinforcement as a function of overburden heights for: a) the strap located at 11.25 ft above L.P in the 52 ft high section, and b) the strap located at 3.25 ft above L.P in the 30 ft high section.

a)

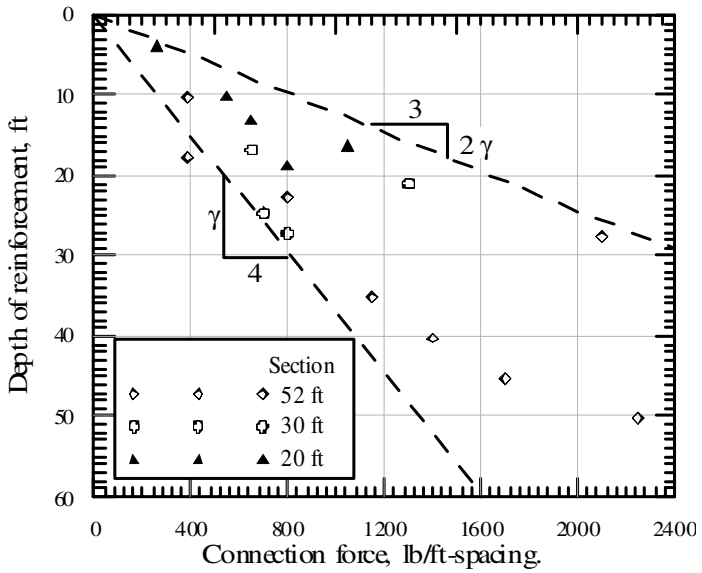

b)

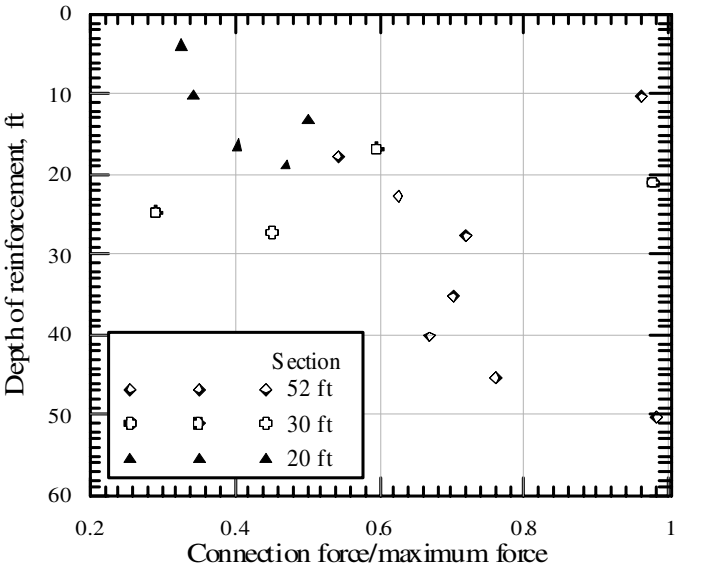

Figure 8 Reinforcement-wall connection forces: a) variation with depth, and b) normalized as a ratio to the maximum reinforcement forces.

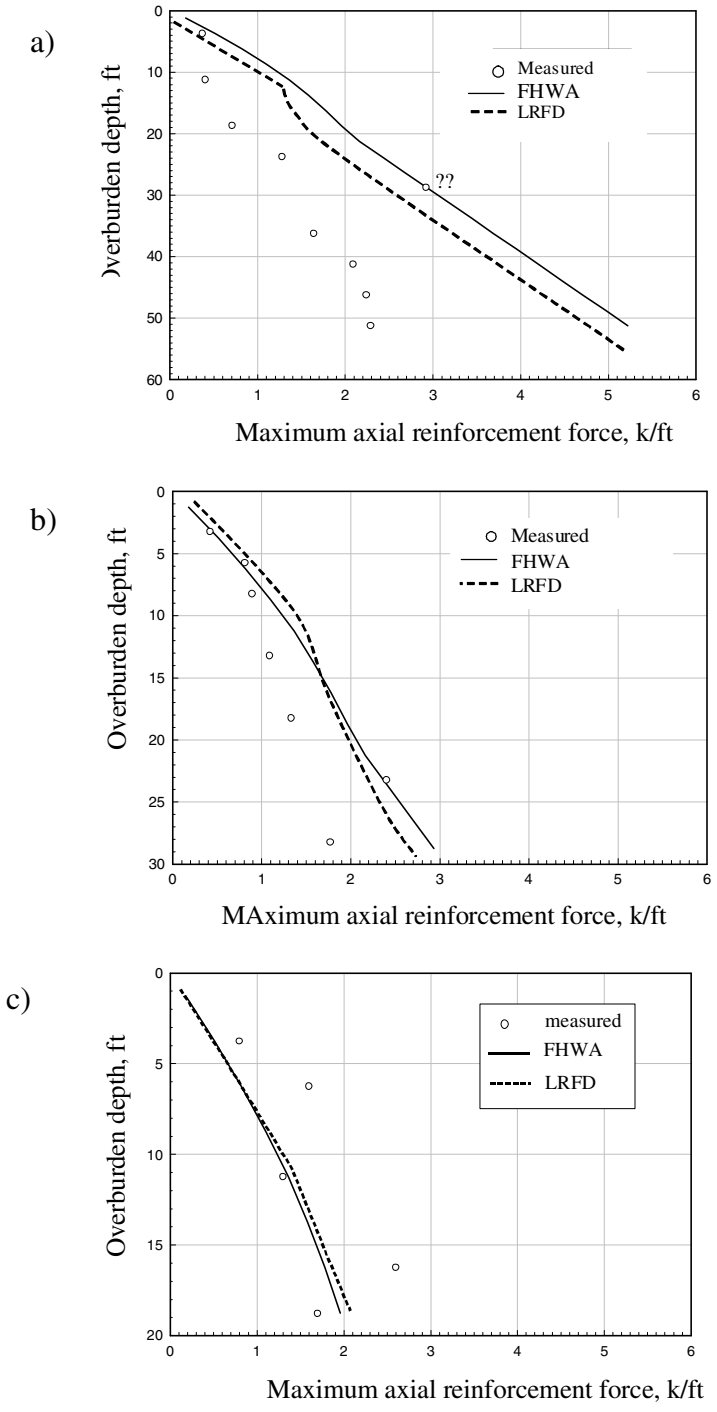

Figure 9 Comparison of the reinforcement maximum axial forces with the FHWA and LRFD methods for the: a) 52 ft high section, b) 30 ft high section, and c) 20 ft high section.

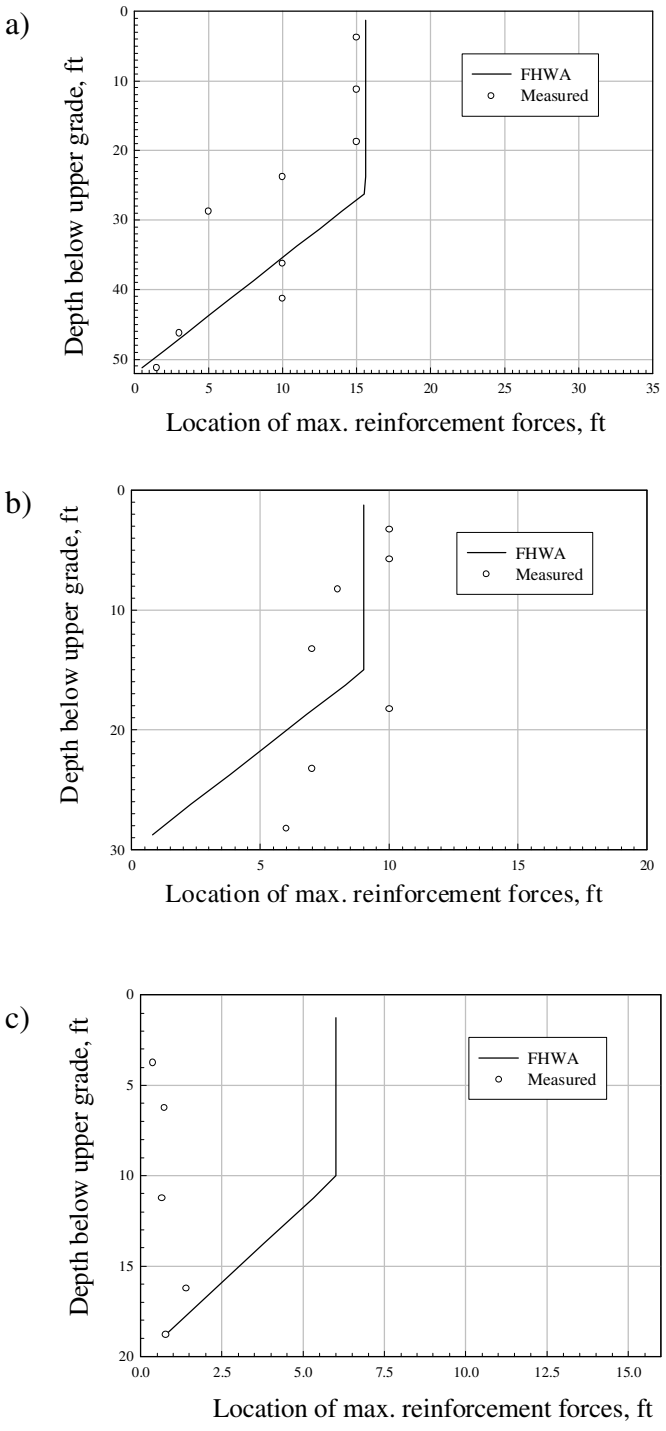

Figure 10 Comparison of the locations of reinforcement maximum axial forces with the FHWA Design manual for the: a) 52 ft high, b) 30 ft high, and c) 20 ft high section.

a)

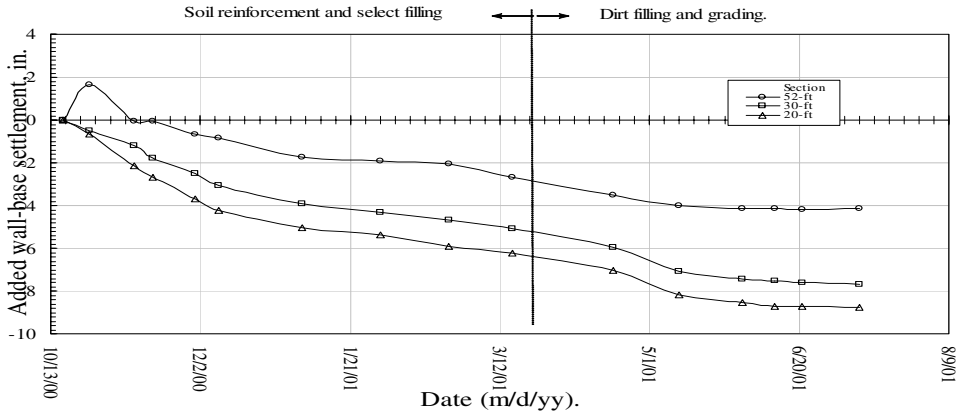

b)

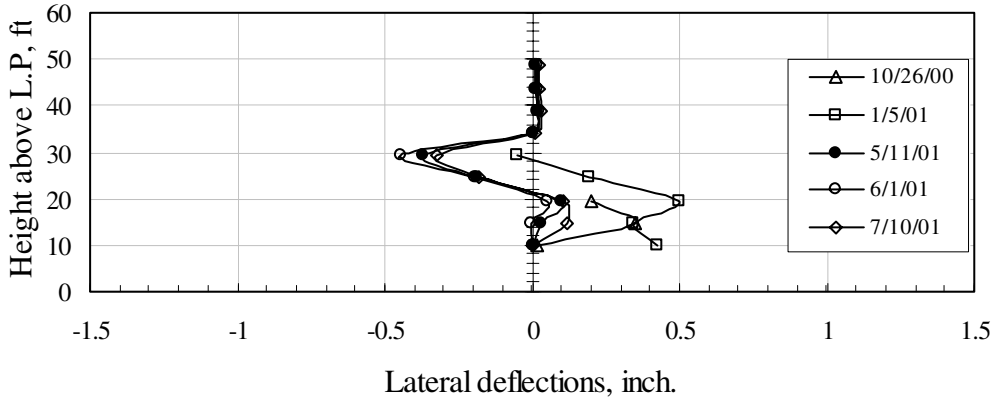

c)

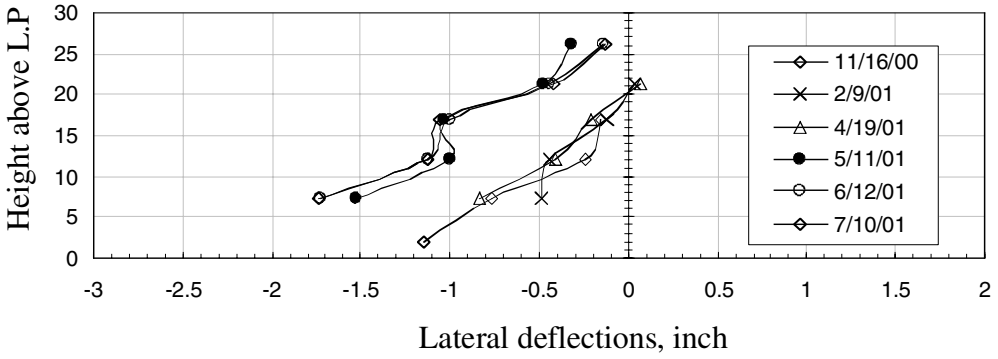

Figure 11 Measured movements of wall facing: a) settlement of wall facing at the instrumented sections, b) lateral deflections at the 52 ft high section, and c) lateral deflections at the 30 ft high section.

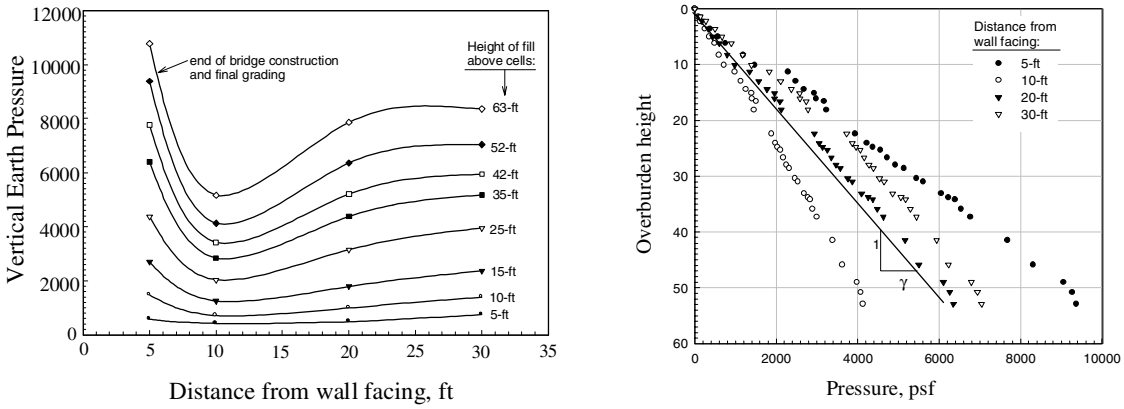

a) **b)**

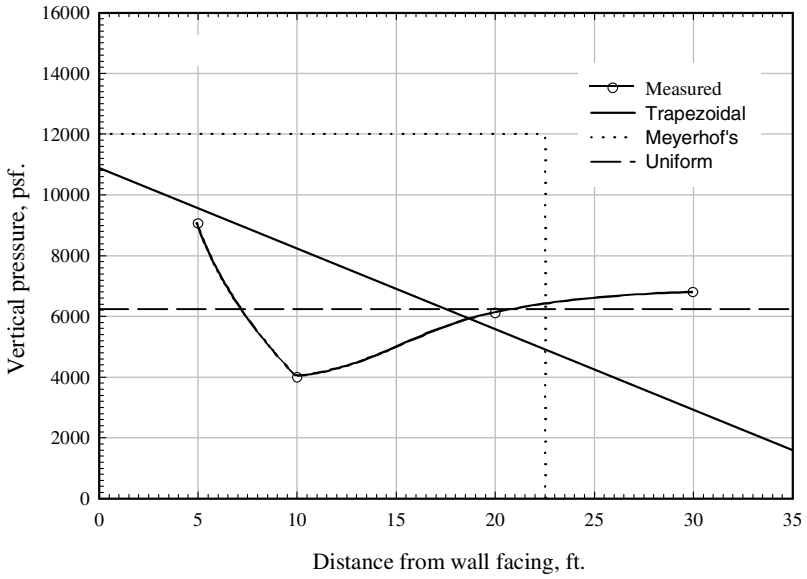

b)

Figure 12 Vertical earth pressure: a) measured profiles along the base of the reinforced soil at different construction stages, b) comparison with geostatic pressure, and c) comparison with commonly assumed distributions.